Single-longitudinal-mode Linear-cavity Er^{3+}-doped Fiber Laser Using Two Subring Cavities

黃堂益 張哲瑄

Abstract: An investigation of single-longitudinal-mode (SLM) Er^{3+}-doped fiber lasers by incorporating double-ring cavities and a section of un-pumped Er^{3+}-doped fiber as a saturable absorber is reported in this paper. The laser is made by an all-fiber linear cavity, composed by a home-made fiber Bragg grating and an optical circulator as the cavity ends. A C-band SLM laser at 1544.7 nm has been successfully achieved with the use of lengthened Er^{3+}-doped fiber having only two subring cavities, inserted either in series or parallel with each other. To the best of our knowledge, it is the first demonstration of a linear-cavity SLM fiber laser based on merely two subring cavities. The SLM laser has a signal to noise ratio of 30.4 dB and its maximum power fluctuation is less than 1.3% for more than 1-hour operation. Such a compact and low-cost system could be of great interest in high-speed and long-haul optical communication**.**

Key words**:** single-longitudinal-mode, fiber laser, subring cavity

Introduction**:** Because of the high-degree of temporal coherence, single-longitudinal-mode (SLM) lasers are of interest in many applications such as optical communication, instrument testing, optical sensors, medical applications and spectroscopy [1,2]. Recently, much more attention has been directed to diode-pumped SLM fiber lasers because of their high reliability, compactness, and capability of shot-noise-limited operation in the megahertz frequency range [3]. Following this research direction, several mode suppression techniques have been investigated in ring cavity fiber lasers [4-7]. Compared with ring-cavity fiber lasers, linear-cavity fiber lasers require fewer intra cavity components and are less expensive, which makes it attractive in various applications. One major problem associated with a linear-cavity fiber laser is spatial hole burning, which enables the oscillation of numerous longitudinal modes and thus prevents the SLM operation. In general, the simplest approach of eliminating the spatial hole burning in the linear-cavity fiber lasers is to ensure that the frequency spacing between two longitudinal modes is greater than the gain bandwidth of gain fibers. For instance, Jeng et al. have demonstrated a single frequency fiber laser with a cm-long laser cavity [8]. However, in such systems, special gain fibers with high rear-earth ion-concentration are required. An alternative way to reduce the number of longitudinal modes is inserting bandwidth-limiting elements inside the cavity [9], and using saturable-absorber for side modes suppression [10,11]. We have demonstrated a linear cavity fiber laser by using Faraday rotator mirror as a cavity end [11]. In this letter, a SLM linear-cavity fiber laser at C-band wavelength is proposed and demonstrated by using only two subring cavities, either in serial or parallel connection. The employed saturable absorber filter and two subring cavities successfully suppress the multi-longitudinal-mode oscillation caused by spatial hole burning in a linear cavity.

***Experimental setup*:** Figures 1(a) and (b) show the experimental setup of the linear cavity SLM fiber lasers with two subring cavities in serial and parallel connection, respectively. The system consists of a backward pumped Er^{3+}-doped gain fiber and a linear fiber cavity, formed at one end by an optical circulator (OC) and at the other end by a lab-made fiber Bragg grating (FBG).

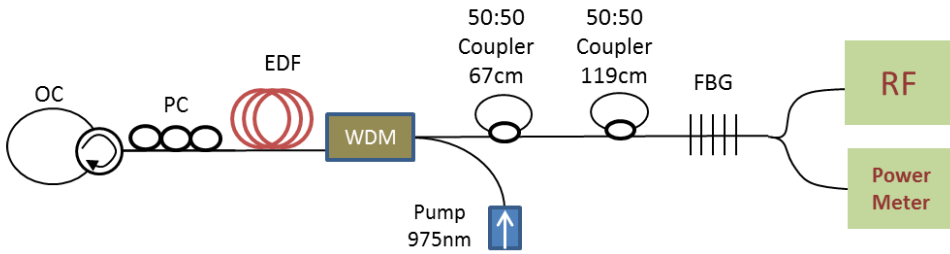

(a)

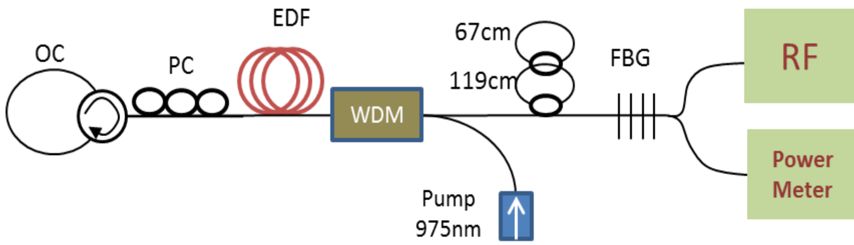

(b)

Fig. 1. Experimental setup of the SLM fiber laser with two subring cavities (a) in series and (b) in parallel connection with each other.

The Er^{3+}-doped gain fiber has a core diameter of 6 μm and Er^{3+} concentration of 2.05×10^{25} ion/m^3. The gain fiber was core-pumped with a wavelength stabilized 50-mW and 975-nm laser diode through a 980/1550 nm wavelength division multiplexing (WDM) coupler. The broadband OC provided reflectivity of 99.28 %. Figure 2 shows the calculated FBG reflectivity versus maximum lasing output power. Based on the parameters indicated in Fig. 1, we find that FBG with low reflectivity may induce large cavity loss; while high reflectivity may induce small portion of output of lasing power. FBG reflectivity at around 40-50% may be the optimal option for maximum power lasing. Therefore, a home-made FBG at 1544.7nm with 3-dB bandwidth of 0.2 nm (25GHz) and

45.7% transmission rate was used in this experiment. The narrow line width FBG could also stabilize the laser wavelength and restrict some longitudinal modes.

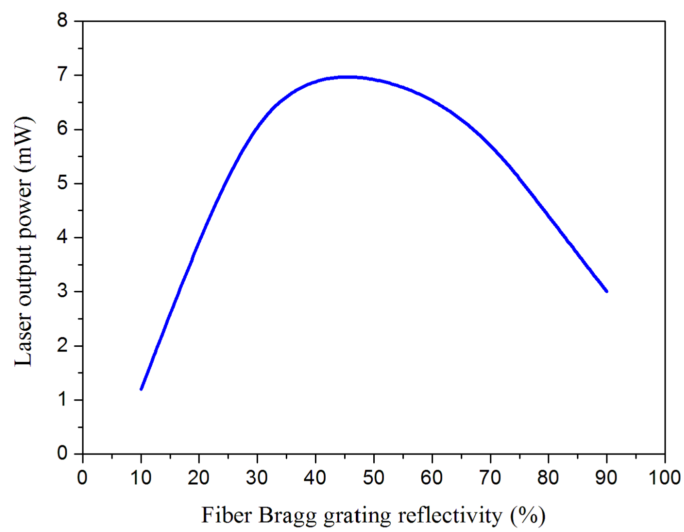

Fig. 2. Fiber Bragg grating reflectivity versus laser output power.

Because the ${}^4I_{13/2}\rightarrow{}^4I_{15/2}$ transition of Er^{3+}in silica fibers is a three-level transition, the Er^{3+}doped fiber can act either as a saturable amplifier or a saturable absorber depending on whether the pump exists. According to Ref. [11], the spatial-hole burning effect in the section of fiber absorber leads to slight refractive index change and generates a weak Bragg grating, serving as a wavelength suppression element. To identify the sections of amplifier and absorber in the employed Er^{3+}-doped gain fiber, we theoretically analyzed the correlation between the residual 975-nm pump and Er^{3+}-doped fiber lengths by using a commercial simulation code LIEKKI™ Application Designer [12]. This code solves the coupled laser rate equations numerically to predict the output performance of the fiber laser sources. It includes the amount of pump power and the required fiber length to achieve a certain output power level, the population inversion at every point along the fiber, the gain spectrum, the forward and backward ASE output powers and spectra, etc.

In addition to the main fiber cavity, two sub-ring cavities in either serial or parallel connection were deployed to restrict furthermore possible longitudinal modes. The effective reflectivity of un-resonant wavelengths inside the subring can be determined by using the equation [13]

$$T = (1-\gamma)^2 e^{-2\alpha L}(1-2k)^2 \tag{1}$$

where T is the transmission of fiber loop reflectors, γ is the insertion loss of the device, α is the fiber propagation loss, k is the split ratio, and L is the fiber length. Each subring cavity was formed by a 50/50 directional coupler. The 50/50 split ratio was selected to provide the highest finesse, resulting in the maximized mode filtering effect. According to Vernier effect for mode suppression, the state of effective free spectral ranges (FSR) becomes the least common multiple number of all cavity FSRs. The polarization controller (PC) inside the cavity is used to align the signal polarization state for fiber laser.

***Experimental results and discussion*:** To experimentally classify the amplifier and absorber sections in the lengthened Er^{3+}-doped gain fiber, we inserted another WDM coupler to extract residual 975-nm pump out from the main cavity and measured the correlation between the residual 975-nm pump and Er^{3+}-doped fiber lengths. As those red dot points shown in Fig. 3, we measured the extracted residual pump power along with the increasing Er^{3+}-doped fiber length, ranging from 0.5 m to 5 m. The black solid curve shown in Fig. 3 was calculated by using the reported values of the fiber parameters, in particular the fiber loss at the pump and signal wavelengths and the cross-section spectra. The results coincide with each other very well, which indicates that there is no 975-nm pump left in the final 2-m fiber. Therefore, the final 2 m of the Er^{3+}-doped fiber can be considered saturable absorber filter.

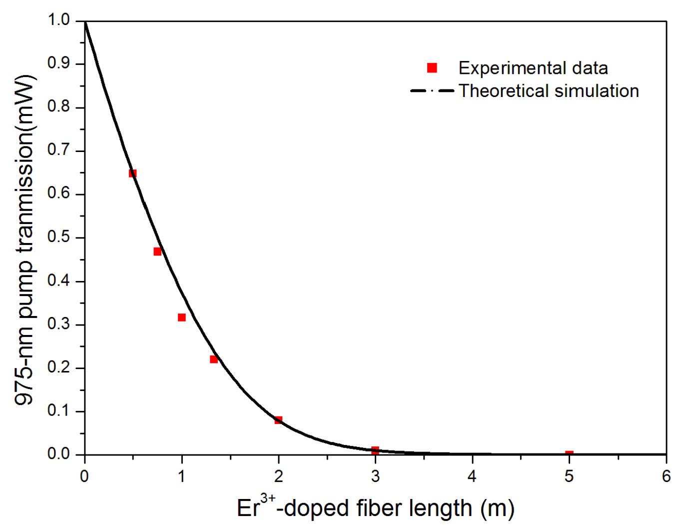

Fig. 3. Measured and simulated pump transmissions for different fiber lengths (dots) under 1544-.7 nm laser operation with pump power of 45 mW.

We measured the laser output power as a function of launched power with the 6-m Er^{3+}-doped fiber as that shown in Fig.4 by using an optical spectrum analyzer (OSA) with a resolution of 0.05-nm. The pump threshold was around 5 mW. The measured laser slope efficiency against pump power was 15.7%. The output spectrum of the fiber laser at an output power of 6 mW is shown in the inset of Fig. 4. It indicates that at the wavelength of 1544.7-nm the laser output spectrum has a signal-to-noise-ratio (SNR) as high as 34.5 dB.

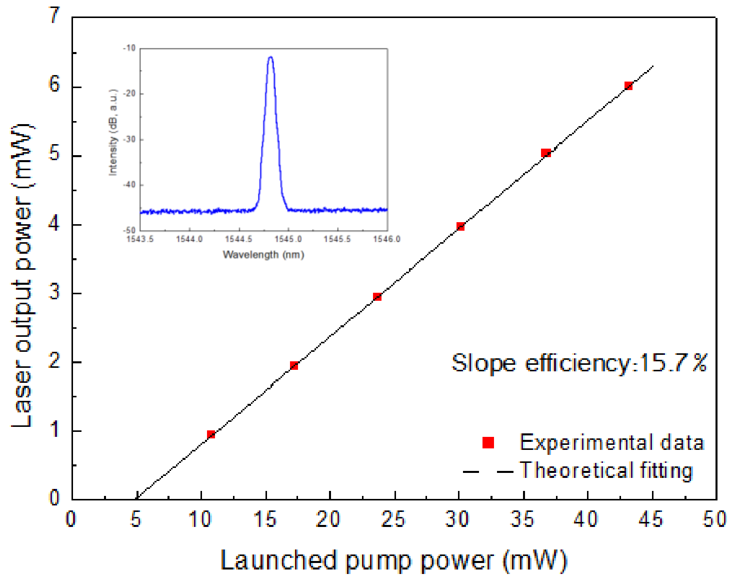

Fig. 4. 1544.7 nm laser power generated by the 6-m Er^{3+}-doped fiber laser as a function of the launched pump power at 975 nm. The inset shows the measured laser spectrum at an output power of 6 mW.

To verify mode suppressing effects of both the saturable absorber filter and subring cavities, we compared the measured RF spectra of the fiber laser with and without the aforementioned mode suppression elements. Using a radio frequency (RF) spectrum analyzer with a resolution of 1 MHz, the laser output spectrum without any subring cavities is shown in Fig. 5. With the 6-m Er^{3+}-doped fiber, the cavity length was measured as 9.8 m, corresponding to corresponding to the free spectral ranges (FSR) of 10.3 MHz. Because of the grating produced by the spatial hole burning in the fiber absorber section, the laser oscillation modes have been modulated with a fluctuation frequency of 90-100 MHz. It is obvious that SLM cannot be reached without the use of subrings in this laser system. Two subring cavities were then inserted inside the cavity in serious and parallel connection with each other. Lengths of the two subring cavities are

67 cm and 119 cm. The resonator modes of the subring cavities should satisfy the following phase condition:

$$kL = 2q\pi, q = 1, 2, 3, \ldots \quad (2)$$

where k is the propagation constant, and L is the length of subring cavity. Therefore, the corresponding FSR of these two subring cavities were of nearly 302.54 MHz and 170.33 MHz, respectively. According to the Vernier effect [13] for mode suppression, the laser mode oscillates only at a frequency that satisfies the resonant condition of each fiber cavity. It means the effective FSR becomes the least common multiple number of all FSR's. In our experiment, at least, two subrings were required to obtain a desired SLM operation. The measured frequency spectra of fiber lasers with the RF spectrum analyzer are shown in Fig. 6(a) with two subring cavities in series connection, and Fig. 6(b) with subring cavities in parallel connection. The line width of less than 1 MHz was successfully achieved in both subring cavity configurations. However, the SLM laser output with two subrings in series connection is not as stable as the one with two subrings in parallel connection. It is because more polarization fluctuation phenomena occurred due to its longer cavity length than that of the parallel-connected scheme. For reliably testing in room temperature, the stable SLM operation can be maintained more than 1 hour with the maximum power fluctuation of less than 1.3%. In a three-level fiber laser, the laser output power increases monotonically with increasing fiber length and reaches a maximum once the pump power is almost absorbed. If the length of gain fiber is increased beyond the optimized value the laser output power starts decreasing due to the signal re-absorption. It was calculated by the code that the maximum laser power can be reached with a 3.5-m gain fiber and the laser power with 6-m gain fiber could be 32% lower than that of the maximum.

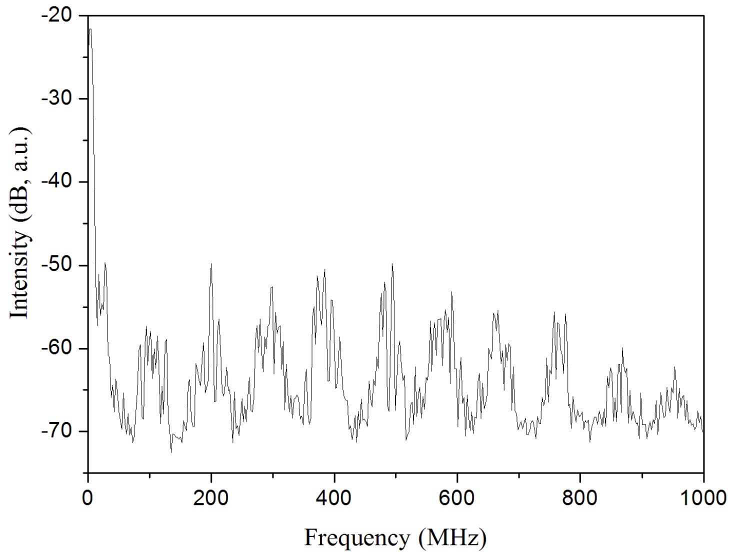

Fig. 5. Measured frequency spectra of the fiber laser without any subring cavity

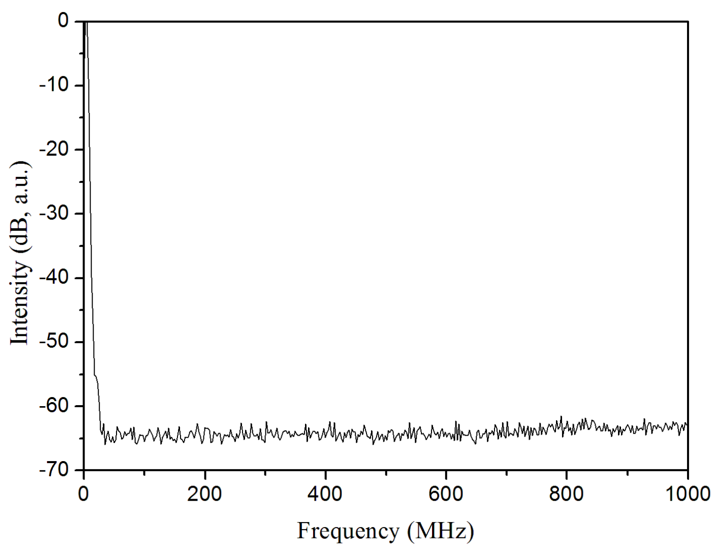

(a)

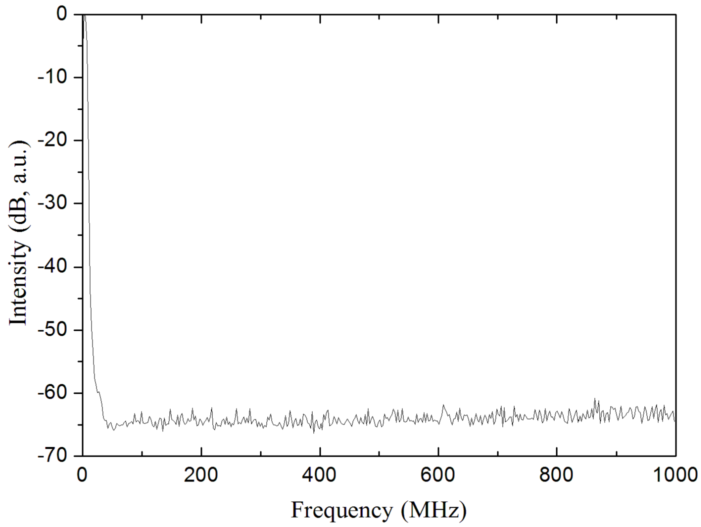

(b)

Fig.6. Measured frequency spectra of the fiber laser with a 6-m EDF and two subring cavities (a) in series and (b) in parallel connection with each other.

Conclusion**:** A simple and compact SLM linear-cavity Er^{3+}-doped fiber laser was proposed and experimentally demonstrated by using only two subring cavities, either in serial or parallel connection. A 1544.7-nm SLM fiber laser with the measured signal-to-noise-ratio of 30.48 dB and line width of less than 1 MHz is successfully achieved. The SLM laser can stably run for more than 1 hour with negligible power fluctuations. Such a laser system could be useful for various applications in long-haul and high-speed optic communication.

Acknowledgment**:** The work is supported in part by NSC of Taiwan under Grand Numbers NSC 102-2221-E-011-088 and NSC101-2218-E-027-003-MY3.

References:

1. C. Spiegelberg, J. Geng, Y. Hu, Y. Kaneda, S. Jiang and N. Peyghambarian, "Low noise narrow line width fiber laser at 1550 nm," Journal of Lightwave Technology, vol. 22, no. 1, pp. 57–62, Jan. 2004.
2. S. P. Bush, A. GüngörandC. C. Davis, "Studies of the coherence properties of a diode-pumped Nd: YAG ring laser," Applied Phys., vol. 53, no.8, pp.646-647, 1988.
3. S. Sanders, N. Park, J. W. Dawson and K. J. Vahala, "Reduction of the intensity noise of a broadly tunable, erbium-doped fiber laser to the standard quantum limit by intracavity spectral filtering," Appl. Phys. Lett. 61:1889, 1992
4. C. H. Yeh, C.W. Chow, Y. F. Wu, Y. H. Lin, B.C. Cheng and J. H. Chen, "Using optimal cavity loss and saturable absorber passive filter for stable and tunable dual wavelength erbium fiber laser in single-longitudinal-mode operation," Laser Phys. Lett., vol. 8, no. 9, pp. 672–677, 2011.
5. Y. Wei and B. Sun, "Wavelength spacing tunable dual wavelength single-longitudinal-mode fiber ring laser based on fiber Bragg gratings," Laser Physics, vol. 19, no. 6, pp.1252-1256, 2009.
6. C.H. Yeh and C.W. Chow, "Broadband wavelength-tunable single-longitudinal mode erbium-doped fiber ring laser using saturable-absorber filter," Laser Phys. Lett., vol. 7, no. 2, pp. 158-163, 2010.
7. F. Wang, E. M. Xu, J.J. Dong and X. L. Zhang, "A tunable and switchable single-longitudinal-mode dual-wavelength fiber laser incorporating a reconfigurable dual-pass Mach–Zehnder interferometer and its application in microwave generation," Optics Communications, vol. 284, no. 9, pp. 2337-2340, 2011.
8. J. Geng, C. Spiegelberg and S. Jiang, "Narrow linewidth fiber laser for 100-km optical frequency domain reflectometry," IEEE Photon. Technol. Lett., vol. 17, no. 9, pp. 1827-1829, 2008.
9. K. Iwatsuki, H. Okamura and M. Saruwatari, "Wavelength-tunable single-frequency and single-polarization Er-doped fibre ring-laser with 1.4 kHz linewidth," Electron. Lett.,vol. 26, pp. 2033-2034, 1990
10. Y. Cheng, J. T. Kringlebotn, W. H. Loh, R. I. Laming and D. N. Payne, "Stable single-frequency traveling-wave fiber loop laser with integral saturable-absorber-based tracking narrow-band filter," Opt. Lett., vol. 20, pp. 875-877, 1995
11. S. K. Liaw, H. Wang, K. H. Hsu, S. C. Lin, N.-K. Chen, C.S. Shin and Y. Tver'yanovich, "Linear-cavity fiber laser in nearly single-frequency operation using Faraday rotator mirror," Laser Physics, vol. 22, no. 2, pp. 437-440, 2012.
12. LIEKKI™ Application Designer, Available online:

http://www.nlight.net/download/lad
13. D. B. Mortimore, “Fiber loop reflectors,” IEEE/OSA Journal of Lightwave Technology, vol. 6, no. 3, pp. 1217–1224, 1988.